

# DC-26 GHz MEMS Series-Shunt Absorptive Switches

Guan-Leng Tan and Gabriel M. Rebeiz

EECS Department, The University of Michigan, Ann Arbor, MI 48109-2122

gtan@umich.edu, rebeiz@umich.edu

**Abstract** The design and performance of a wideband coplanar waveguide (CPW) DC-26 GHz MEMS absorptive switch on silicon substrate is presented. The absorptive switch utilizes novel DC-contact series and shunt fixed-fixed beam MEMS switches with 'dimples' at the contact area for improved contact resistance. An insertion loss of 0.5 dB or better is achieved from DC-26 GHz. The isolation is -40 dB at 5 GHz, -35 dB at 10 GHz and -25 dB at 26 GHz. These switches are useful in applications where good return loss is required in the isolation state.

## I. INTRODUCTION

Solid-state-based switches are a mature technology which find widespread application in commercial and military systems. These switches have excellent switching speed and wide bandwidth [1], but they have a relatively high DC power consumption which render them unsuitable for applications requiring a large number of switching elements, such as in electronic scanning arrays. Micromachined switch technology is rapidly gaining acceptance as an enabling technology in such high-performance systems due to the low power consumption and excellent insertion-loss and isolation performance of MEMS switches.

The series-shunt design is a well-established configuration for achieving wide bandwidth in solid-state switches, with excellent performance that extends down to DC. In the case of MEMS, however, the series MEMS switch is typically a DC-contact design [2]-[3], while the shunt MEMS switch is a capacitive switch. Since the isolation of the switch is determined by the shunt switch, in order to achieve good performance at low microwave frequencies, the shunt switch must also be a DC-contact type. Furthermore, the series and shunt switches must be individually biased and connected to matched resistors. This paper presents a wideband absorptive switch with all these desired characteristics.

## II. DESIGN

The wideband absorptive switch is designed using two MEMS DC-contact series switches and an in-line shunt DC-contact switch. A  $50 \Omega$  tantalum nitride resistor is connected across the gap of each series switch. The resistor is shorted when the switch is actuated, providing a low-loss path from the input to output ports. The switches are cascaded together using short lengths of transmission lines, resulting in a configuration shown in Fig. 1, with the shunt switch placed between the two series switches.

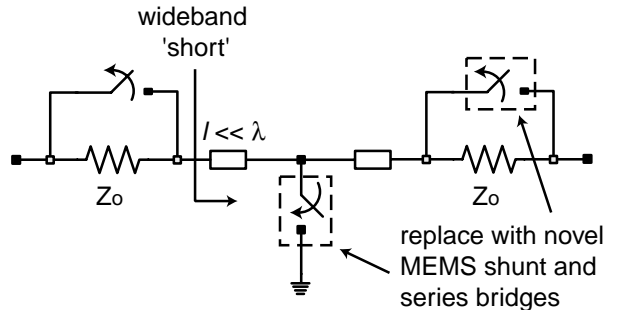


Fig. 1: Wideband MEMS absorptive switch configuration.

Both the series and shunt switch elements used are based on a fixed-fixed beam design (Fig. 2). The series switch is an all-metal design [4]. This results in a fabrication procedure which is compatible with the fixed-fixed beam shunt switch. The disadvantage is a slightly higher capacitance in the up-state position. All switches have thick electroplated anchors (3  $\mu\text{m}$ ). This yields an effective anchor-to-anchor bridge length of 270  $\mu\text{m}$ . The bridges are placed in a CPW line configuration on a 400  $\mu\text{m}$  silicon substrate with  $W = 160 \mu\text{m}$  and  $G = 100 \mu\text{m}$ . A bridge width of 100  $\mu\text{m}$  is used in all the bridges. For the series switches, sputtered  $50 \Omega$  tantalum nitride resistors are placed across the 40  $\mu\text{m}$  gaps, under the bridges.

The pull-down electrodes are placed close to the anchors rather than at the center of the bridge, where

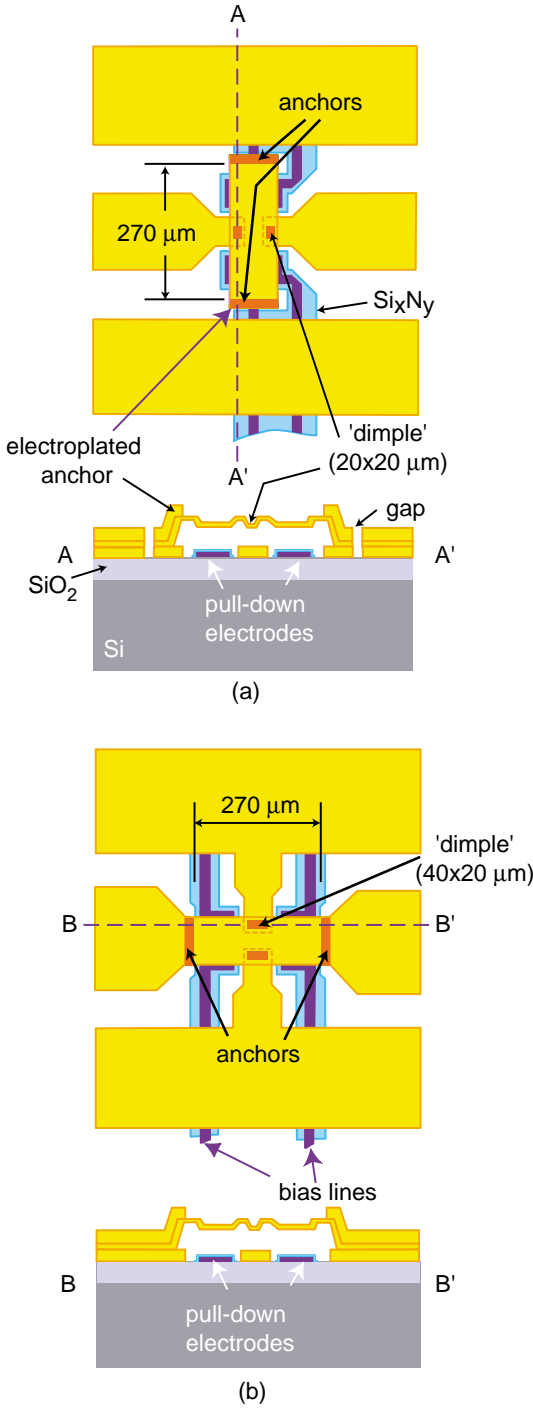


Fig. 2: Novel fixed-fixed beam DC-contact switches used in the absorptive switch design: (a) series switch, and (b) shunt switch.

the contact areas are located. They are isolated from the bridge using 2000 Å PECVD silicon nitride. The bias lines are brought underneath the ground plane to an external bias pad using the same nitride passivation. In addition, a 2  $\mu$ m silicon dioxide layer is deposited on top of the bias lines under the ground plane to decrease the capacitive coupling to the ground planes. The bias lines are made of a high resistivity material (sputtered SiCrN, with about 1400  $\Omega$ /square sheet resistance). A high sheet resistance is critical for achieving a low insertion loss since the series bridges are directly connected to the bias lines.

In order to ensure a good DC-contact, a 'dimple' in the bridge 6000 Å-deep is designed for each contact point. When the bridge is pulled down, the dimple makes contact with the ground plane (shunt switch) or the transmission line (series switch), but there is only minimal contact at the pull-down electrodes, unless a voltage significantly higher than the actuation voltage is applied. This helps to alleviate stiction problems.

The absorptive switch is in the insertion-loss state when the two series switches are actuated (down-position) and the shunt switch is in the up-position (Fig. 3(a)). In this state the shunt switch has a small capacitive coupling to the CPW ground. This coupling is minimized by introducing a gap in the overlapping area under the bridge. Two slightly inductive lines (62  $\Omega$  impedance) are used for the interconnecting lines between the series and shunt bridges to offset the effect of the up-state capacitance of the shunt bridge for good return loss.

The isolation-state is activated when the in-line shunt bridge is brought to the down-position, shorting the input signal to CPW ground. Good return loss is obtained by leaving the series switches in the up-state, so that each port is effectively connected to a 50  $\Omega$  termination through the short at the shunt bridge. The equivalent circuit in the isolation state is shown in Fig. 3(b).

The fabricated circuit is shown in Fig. 4. Also shown in the figure are the measurement reference planes.

### III. MEASUREMENT AND DISCUSSION

The wideband switches are measured using HP 8510C network analyzer with a wideband TRL calibration. Bias is applied to the pull-down electrodes using needle probes, and the MEMS bridges are kept at ground potential using a bias-T in the case of the shunt switch, and using the resistive bias lines in the case of the series switches. The measured pull-down voltage for a reliable contact is 30-35 V.

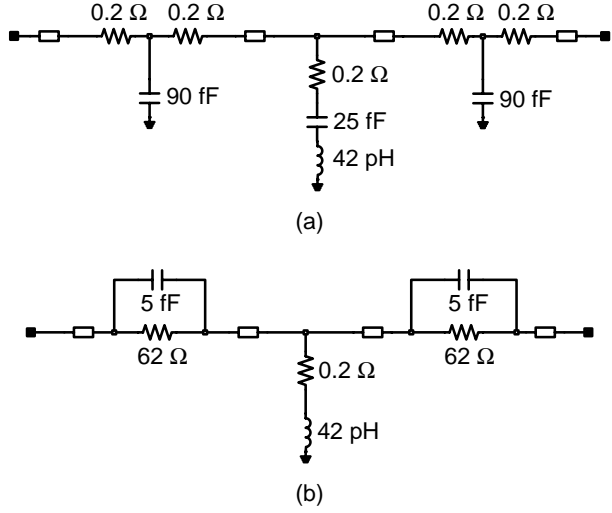


Fig. 3: Simplified equivalent circuit of the absorptive switch in the (a) insertion loss state and (b) isolation state.

The measured results for the switch in the insertion loss state is shown in Fig. 5. The switch achieves an insertion loss of 0.5 dB or less from DC-26 GHz. The curve-fitted equivalent circuit using Libra [5] is shown in Fig. 3(a). Note that the two all-metal series bridges are in the down-state position, and therefore each appear as a balanced pair of open stubs with an equivalent capacitance of 90 fF. These 'stubs' are responsible for the shape of the return loss response. The low-frequency insertion loss of the switch is limited by the contact resistance of the series switches. For the present design, the measured results corresponds to an RF series resistance of 0.2 Ω per contact (there are two contacts per series switch). The measured DC contact resistance is about 0.35 Ω per contact. The measured return loss of the switch is better than -12 dB from DC-26 GHz.

The isolation-state performance of the wideband absorptive switches is shown in Fig. 6. The isolation bandwidth of the switch is primarily determined by the quality of the 'short' at the DC-contact shunt switch. In this design, there is an equivalent inductance of 42 pH from the ground plane connection ( $l_g$  in Fig. 4) which degrades the "short" as frequency increases, resulting in a degradation in isolation with frequency. However, the isolation of the switch is -23 dB at 26 GHz and better than -37 dB below 10 GHz, which is excellent.

The return loss of the switch in the isolation-state is at least -10 dB below 20 GHz. The return loss

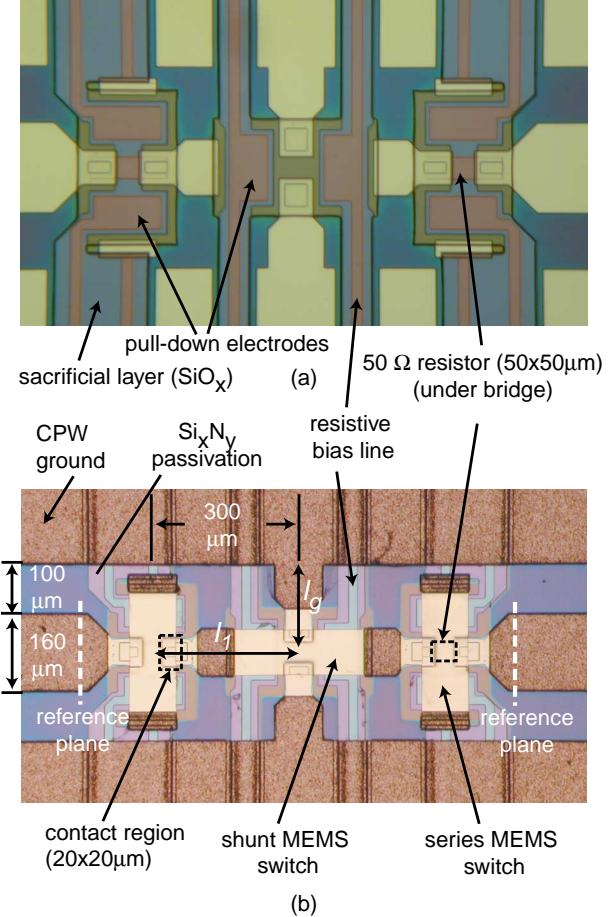


Fig. 4: Photographs of the wideband MEMS absorptive switch: (a) after deposition of sacrificial layer; (b) complete switch.

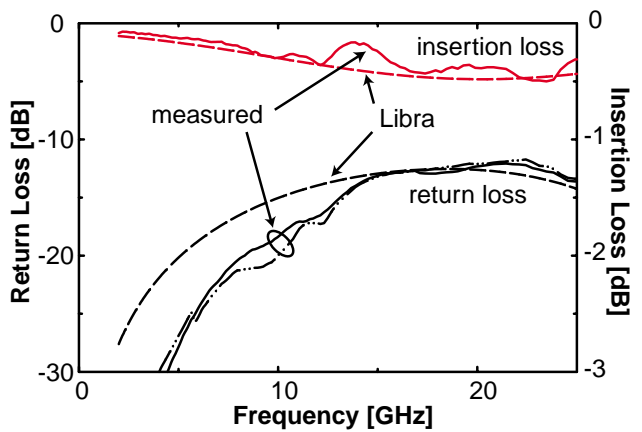


Fig. 5: Simulated and measured performance of the absorptive switch in the insertion-loss state.

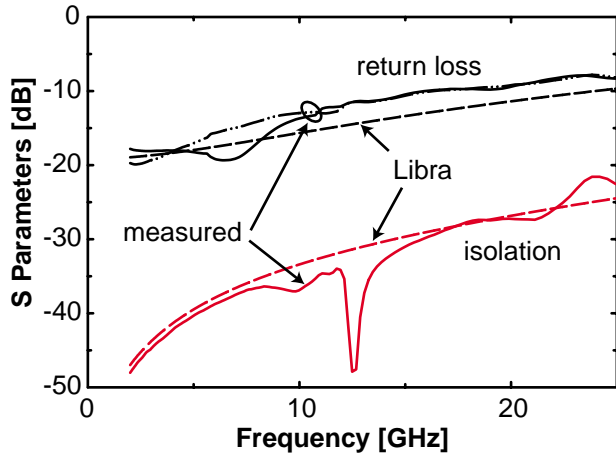


Fig. 6: Simulated and measured performance of the absorptive switch in the isolation state.

at low frequencies is limited by the deviation from  $50\ \Omega$  in the fabricated resistors. The measured results corresponds to  $62\ \Omega$  resistors.

The high-frequency return loss is dependent on the distance  $l_1$  and  $l_g$  between the absorbing resistors and the "short" to ground (Figs. 4 and 7). Reducing  $l_1$  and  $l_g$  improves the "short" at the matching resistors when the shunt switch is closed, thereby improving the return loss. Therefore in order to achieve the widest possible isolation-state reflection bandwidth, it is important to minimize the path length from the resistor to ground.

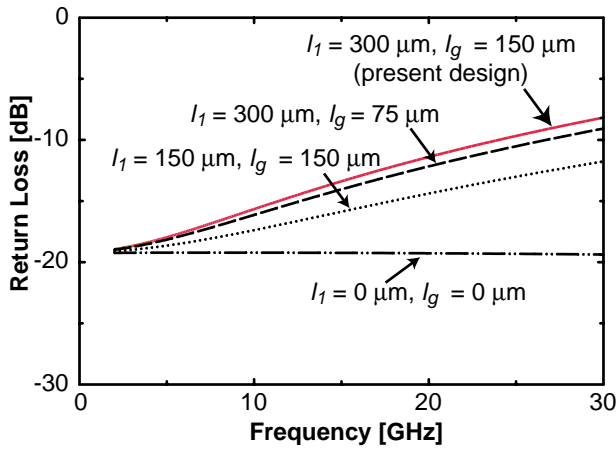


Fig. 7: Effect of  $l_1$  and  $l_g$  on absorptive switch return loss bandwidth in the isolation state ( $R=62\ \Omega$ ).

#### IV. CONCLUSION

A wideband MEMS absorptive switch based on the series-shunt approach has been successfully designed and fabricated for DC-26 GHz operation. Novel DC-contact switch elements have been used to implement the switch. The limitation on the bandwidth is evaluated and found to be due to the inductances associated with the layout.

#### ACKNOWLEDGEMENT

This work is supported by the DARPA RECAP program.

#### References

- [1] Mizutani H., Funabashi N., Kuzuhara M., Takayama Y., "Compact DC-60-GHz HJFET MMIC switches using ohmic electrode-sharing technology," *IEEE Transactions on Microwave Theory and Techniques*, vol. 46, no. 11, Nov. 1998, pp.1597-1603.
- [2] M. Kim, J. B. Hacker, R. E. Mihailovich, J. F. DeNatale, "A DC-to-40 GHz four-Bit RF MEMS true-time delay network," submitted to *IEEE Microwave and Guided Wave Lett.*
- [3] Personal Communications, Bob Loo and Clifton Quan, HRL.
- [4] Jeremy B. Muldavin and Gabriel M. rebeiz, "Novel series and shunt MEMS switch geometries for X-Band applications," *30th European Microwave Conference*, vol. 1, Oct. 2000, pp.260-263.
- [5] HP Co., Santa Clara, CA, HP EESof Communications Design Suite v 6.1, 1996.